DISTRIBUTION STATEMENT A. Approved for public release; distribution is unlimited.

Transport of Gas and Solutes in Permeable Estuarine Sediments

Markus Huettel
Department of Earth, Ocean and Atmospheric Science
Florida State University,
117 N Woodward Ave.
Tallahassee, Florida, 32306-4320, USA
phone: (850) 645-1394 fax: (850) 644-2581 email: mhuettel@fsu.edu

Award Number: N00014-08-1-0360
http://myweb.fsu.edu/mhuettel/

LONG-TERM GOALS

The long-term goals of this project are to 1) quantify gas bubbles and their composition in shallow nearshore marine sand and 2) to assess the role of gas bubbles in shallow sandy coastal sediment for the transport of solutes through the sand and sediment-water exchange of matter. Due to their compressibility, gas bubbles embedded in shallow water sediments cause interstitial water oscillations under passing surface gravity waves, and these oscillations provide a mechanism for enhanced solute dispersion and flux.

OBJECTIVES

1) To detect gas bubbles and in coastal and estuarine sand deposits and to assess temporal and spatial distribution of sedimentary bubbles in sublittoral beds including sands inhabited by microphytobenthos and seagrass.
2) To quantify the size range and composition of the gas bubbles in the sediment and the overlying water.
3) To determine the volume change and migration velocities of interstitial bubbles and the links to pressure oscillations
4) To assess dispersion and transport of solutes caused by bubble volume change and migration under different pressure conditions.

APPROACH

The project combines instrument development with laboratory and field measurements.

– Instrument development initially focused on a **hand-held ultrasound device for the detection of small gas bubbles** embedded in sandy sediment. This device was tested in the laboratory and in the field, and was deployed for the detection of small bubbles produced by photosynthesis in sublittoral sands.

- In the second phase of the project, we initiated the construction of a **laboratory column reactor that allows application of realistic pressure oscillations to incubated sediment cores** with gas enclosures.
- **Field measurements** combined the detection and measurement of gas release volumes from sandy sediments using benthic chambers and bubble traps. While the chambers allowed changing the advective transport component and thereby also gas ebullition, the bubble traps collected bubbles under the natural flow conditions. The composition of the sampled gas volumes is analyzed using a Gas Chromatograph (GC).
- **Gas stripping experiments** were conducted in laboratory column reactors filled with natural sands and in the field using gas injection techniques that test the gas stripping caused by nitrogen and methane ebullition.
- **Measurement of gas bubble dimensions and distribution**. Bubble size analyses were performed using ultrasonic and optical methods on sediment cores maintained at in-situ pressure, light and temperature and without changing the orientation of the core.
- **Mapping of the spatial and temporal distribution of high sedimentary photosynthetic production and sites for free gas development.** Measurements with an in-situ fluorescence detector and an the acoustic detector were used to map areas of benthic photosynthetic bubble production.
- **Determination of gas content, distribution and migration in the surface sediment.** Content, distribution and migration of free gas in the surface layers of the sand sediment was investigated with a tunable ultrasound square wave pulser, with measurement rate adjustable from 10 Hz to 1000 Hz in 10 Hz increments connected to one sending and one receiving high-frequency transducer (1 MHz).
- **Measurement of solute transport caused by bubble compression and migration.** This process was investigated in the field using benthic chambers and a laboratory column setup which allowed measurement of the migration behavior and velocities of gas bubbles in permeable sandy sediments under the influence of sinusoidal pressure oscillations and determination of transport rates, dispersion and interfacial flux of solutes and colloidal material.

For a more detailed description of the methods and technologies used in this project and results in the previous years we refer to the first three annual reports. Below a summary of the work completed within the reported project year 2010/2011.

WORK COMPLETED

Testing of the acoustic detection method for measuring the speed of sound

The velocity of sound in sediment can be used to characterize sediment layers, i.e. the reflectivity of individual sediment layers. We tested the ability of our new acoustic bubble detection method for measuring the speed of sound in the sand. A solid reflector was embedded in the sediment at a defined depth and then a set of reference measurements was recorded in pulse echo mode with the submerged 1MHz transducer positioned 2 cm above the sediment-water interface. Temperature of the water was kept constant at 22 C. The the recorded waveform data are downloaded onto a PC computer and imported into a spreadsheet program that permited plotting of the data. The acoustic records contained series of paired time (in µs) and reflection intensity (in V). Time periods between reflection peaks

produced at boundaries between reflector were used to calculate sound velocity in water and sediment. Two characteristic numbers for each acoustic profile are calculated: 1) the total reflectivity and 2) the center of reflection. Total reflectivity is given by the sum of reflection amplitudes (A_R, with units of V) of the sediment section of the acoustic profile for the selected time interval (which corresponds to a depth interval). Differences in the mean A_R value for different replicate sets imply changes in the amount of sound energy reflected from the sediment depth interval. The calculation of the center of reflection intensities (C_R, with units of μs) is defined as the average travel time weighted by the magnitude of the individual reflection signals:

$$C_R = \frac{\sum_{i=m}^{n} V_i t_i}{\sum_{i=m}^{n} V_i} \qquad (1)$$

where m and n are the starting and ending datum points for the chosen time interval (again corresponding to a depth interval), and V_i and t_i are the voltage and time since the initial pulse at a given datum point, respectively. The speed of sound was calculated from the travel time of the sound pulses between transducer and sediment surface (velocity in water) and between sediment surface and the embedded solid reflector.

Acoustic mapping of bubbles in sand sediments

Field measurements were carried out in St. Joseph Bay, FL (29°50’43.30” N, -85°19’45.38” W), to map small sedimentary bubbles in shallow sand sediments colonized by photosynthetizing diatoms and cyanobacteria. Photosynthetically active radiation at the water surface raged from 1000-2000 μEinstein m^{-2} during the measurement period. Acoustic readings were collected in two sand areas (~300 cm^2 each) separated by 50 cm. Sand from the upper 10 cm and even deeper layers of shallow sands typically is photosynthetically active when exposed to light. For two dimensional plots of sedimentary sound reflection, acoustic profiles were vertically aligned using the reflection of the sediment-water interface as reference depth. Sound travel times were converted to distances and all peaks equal or smaller than the average background noise level were removed from the measured profiles.

Quantification of bubble release volumes and composition

Gas collectors (Fig. 1), 0.5 m in diameter and made of transparent foil, were deployed in shallow water (~1m) to capture photosynthetically-produced bubbles and quantify gas volume and composition throughout day/night cycles during winter, spring, summer and fall 2011. Gas samples were stored in gas-tight vials and measured on a Shimadzu gas chromatorgraph-8A TCD for oxygen and nitrogen percentages. In addition, sediment samples were collected and free gas was extracted through gentle resuspension of the sediment and trapping of emerging bubbles.

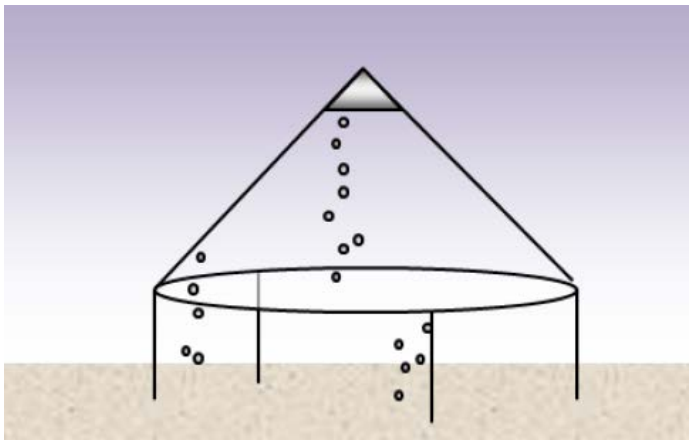

Fig. 1 Gas traps used for quantification of ebullition gas. Diameter of the traps was 0.5 m. Six of these traps were seasonally deployed on a 10 m^2 area in shallow water at St. Josephs Bay/Florida. Gas was extracted from the apex of the trap with gas tight glass syringes.

Assessment of bubble response to pressure oscillations

Gas bubbles in the millimeter-size range were introduced in our water-filled pressure control column and exposed to sinusoidal wave pressure oszillations. The oscillating compression of the bubble was documented via high-frequency digital imaging. The individual pictures were analyzed using an image analysis software producing calibrated bubble volumes for known pressures (Fig. 2).

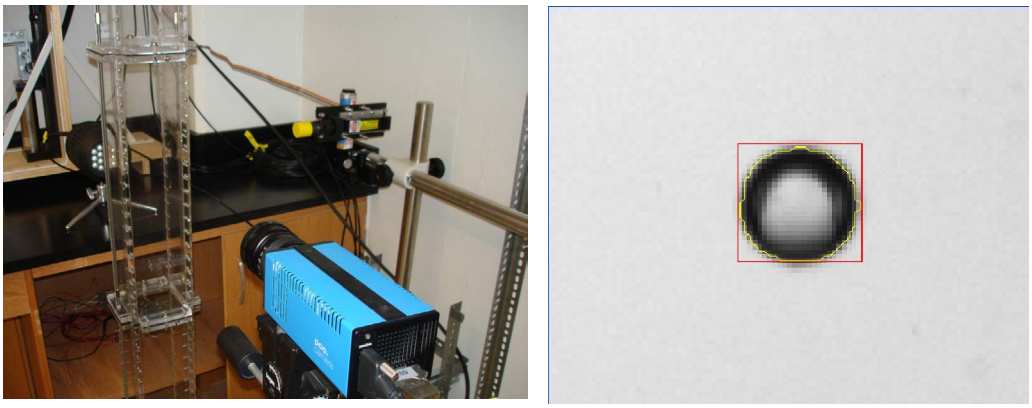

Fig. 2. Left: Setup of pressure column with high speed camera. Right: Millimetre-size bubble with automized measureing frame used to quantify bubble volumes. The image analysis program uses the color gradient to outline the bubble.

Assessment of sedimentary bubble response to pressure oscillations

In a similar experiment, a bubble was introduced 5 cm deep in saturated sand (250 um grain median) and exposed to pressure oscillations of 20 kPa. The resulting oscillation of the bubble volume was assessed through image analysis.

RESULTS

Testing of the acoustic detection method for measuring the speed of sound

Sound speed in water measured with our method ranged from 1476-1590 m s^{-1} with a mean of 1523 m s^{-1} (SD = 32 m s^{-1}) (Table 1). Thes values agree with the published range (Wille 2005). Laboratory tests suggest that the acoustic wave speed in water-saturated sand (S_s) is dependent on frequency (Turgut and Yamamoto 1990; Williams 2002) and for 1 MHz sound S_s is ~1770 m s^{-1}. This agrees well with our measurements, which ranged from 1548-2294 m s^{-1} (mean = 1799 m s^{-1}, SD = 203 m s^{-1}). The propagation of sound through saturated sand is also dependent on particle size. Consequently, while our results may not be directly comparable to previous studies of continental shelf sands because of our higher sound frequencies and different grain size distributions, our values of S_s are on par with other published values: 1650 m s^{-1} (Knobles et al. 2006), 1680 m s^{-1}(Hines et al. 2010), 1760, 1800 m s^{-1} (Thorsos et al. 2001), and 1780 m s^{-1} (Hefner et al. 2009).

Acoustic mapping of bubbles in sand sediments

Acoustic scans of the sands measured in the early morning prior to intense illumination show only a few small inhomogeneities in the spatial distribution of relative reflection intensity values (Fig. 3). After exposure to strong midday sunlight, larger reflecting areas in the uppermost 10 mm of the sand developed that disappeared after the sediment was mixed leading to the release of gas bubbles. The contour plots show that the acoustic method can detect zones of different acoustic impedance on the millimeter depth scale. Below the upper 10 mm, thin horizontal layers (< 10 mm) of increased relative reflection intensity indicate layers of different compaction or grain size distribution (e.g., storm layers). Bubbles produced by benthic photosynthesis also occurred below 3 mm sediment depth, considered the maximum depth to which light penetrates saturated quartz sand (Kuehl and Joergensen 1994). (De Beer et al. 2005; Werner et al. 2006; Jansen et al. 2009), and others have shown that oxygen supersaturation in the pore water of shallow water sands caused by benthic photosynthesis can reach much deeper (up to 20 mm) than light penetration into the sand. In highly permeable sands as present at our study sites, advective pore water flows and molecular diffusion transport oxygen below the photosynthetically active sediment layer (Huettel and Rusch 2000). Supersaturated pore water carried deeper into the sediment by advective pore water flows and an increase of sediment temperature triggered bubble formation at depth below light peneteration in the sand. This mechanism is supported by our laboratory experiments described in the previous report. Such bubbles below the photosynthetically active layer should affect sediment biogeochemical processes as they may function as temporary reservoir for oxygen, extending aerobic microbial processes in space and time.

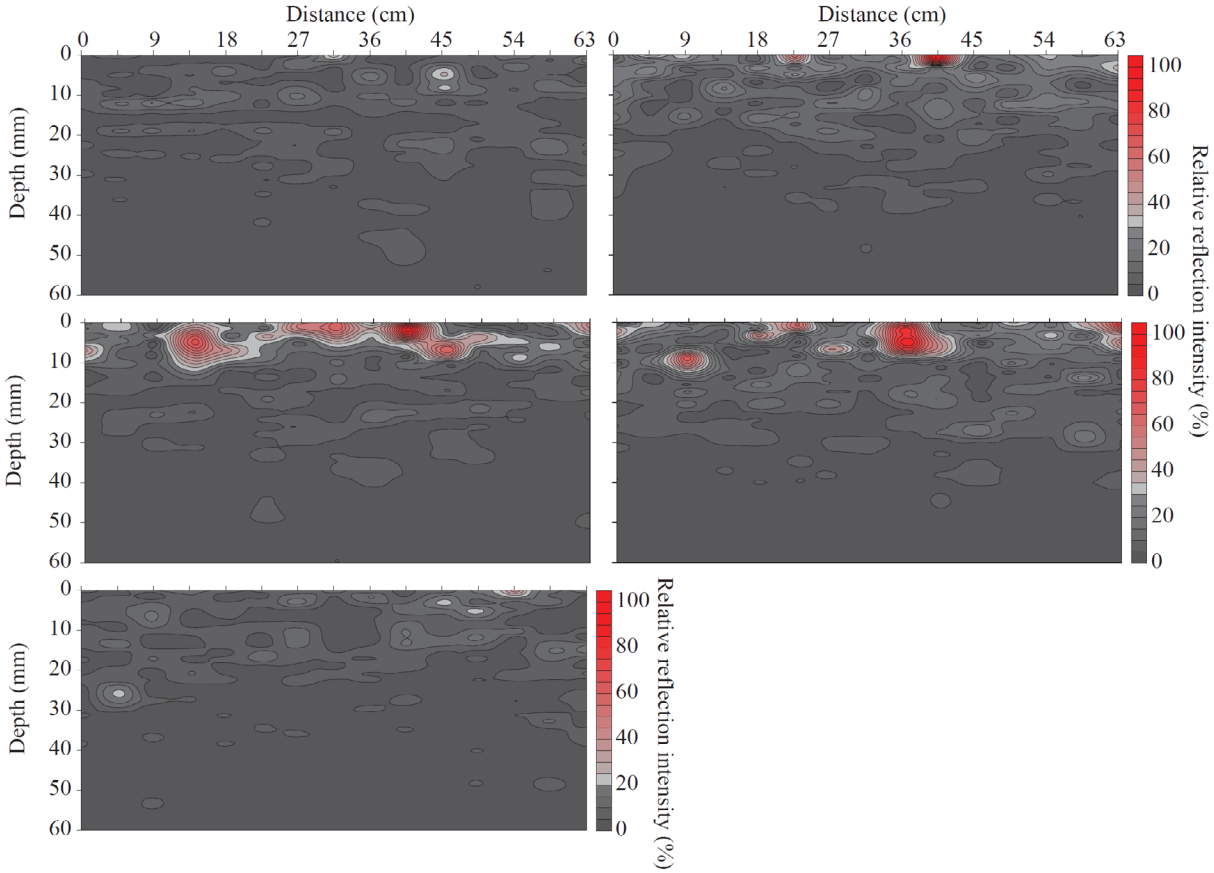

Fig. 3. Acoustic scans conducted at St. Joseph Bay, Florida. The three left panes represent Site 1 upper pane: shortly after sunrise, middle pane: after 3 h sunshine, lower pane: after sunshine and overturning of the sand. The two right panes represent Site 2: upper pane: initial setting without bubbles, lower pane: after 1.75 h of sunshine.

Quantification of bubble release volumes and composition

Gas volumes collected in February 2011 were about one order of magnitude smaller than during May 2011, although sediment chlorophyll a concentrations were not significantly different (Fig. 4). Lower light intensities and temperatures in February limited photosynthesis, and the colder water could dissolve more oxygen. Dinoflagellates were the dominant sedimentary photosynthesizing group in February but absent in May, where mainly the diatom groups dominated. During both sampling periods, highest ebullition occurred during evening and night hours. Oxygen built up during daylight hours, and bubbles formed in the sediment. In February, gas samples were only found and collected in the traps past 18:00 hours with samples containing between 20 to 30% oxygen. Sediment analyzed for free gas content contained approximately 2 ml of gas with about 40% oxygen. In May, sedimentary gas production was higher (up to 150 ml) and gas was also found during daytime (4-30 ml m^{-2}) although night samplings produced higher volumes. Average gas volumes and oxygen content were greatest at 18:00 (89 ml and 55%). Little or no gas was observed in either season in the sediment at morning 6:00 time points; the period with minimal ebullition. Despite smaller gas volumes in sediment, O_2 content was typically higher than in the gas traps. The key result was that gas bubbles that built up during the day in the sediment were released during the dark period providing a transport and aeration mechanism during the time when photosynthesis was not active.

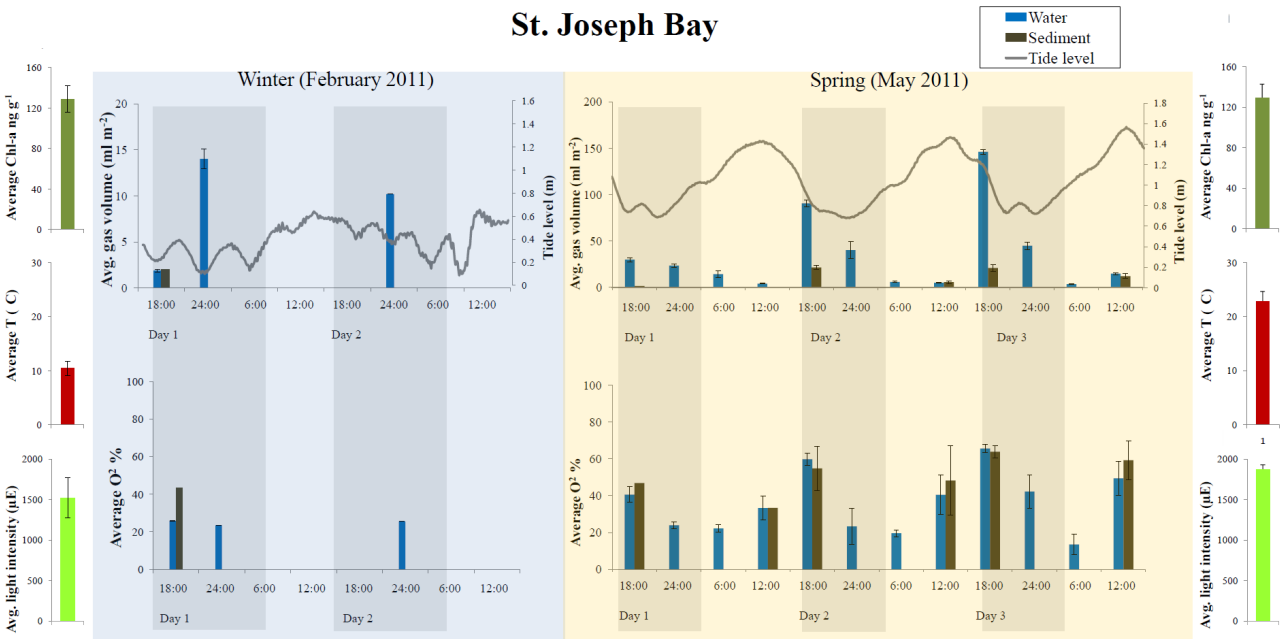

Fig. 4. Results from gas traps from the winter and spring deployments. Upper graphs: gas volumes in traps and sediment cores. Lower graphs: Oxygen content in gas samples. Side panels give average chl-a concentration, water temperature and light.

Assessment of small bubble response to pressure oscillations

Small bubbles subjected to pressure oscillations caused by surface gravity waves showed an oscillation in volume inversely proportional to the pressure (Fig. 5). For pressure oscillations in the 20 kPa range, corresponding to waves with a height of 2 m (amplitude 1 m), the volume change of 2 mm^3 bubbles reached 15%. The volume change showed a pronounced hysteresis with faster compression of the

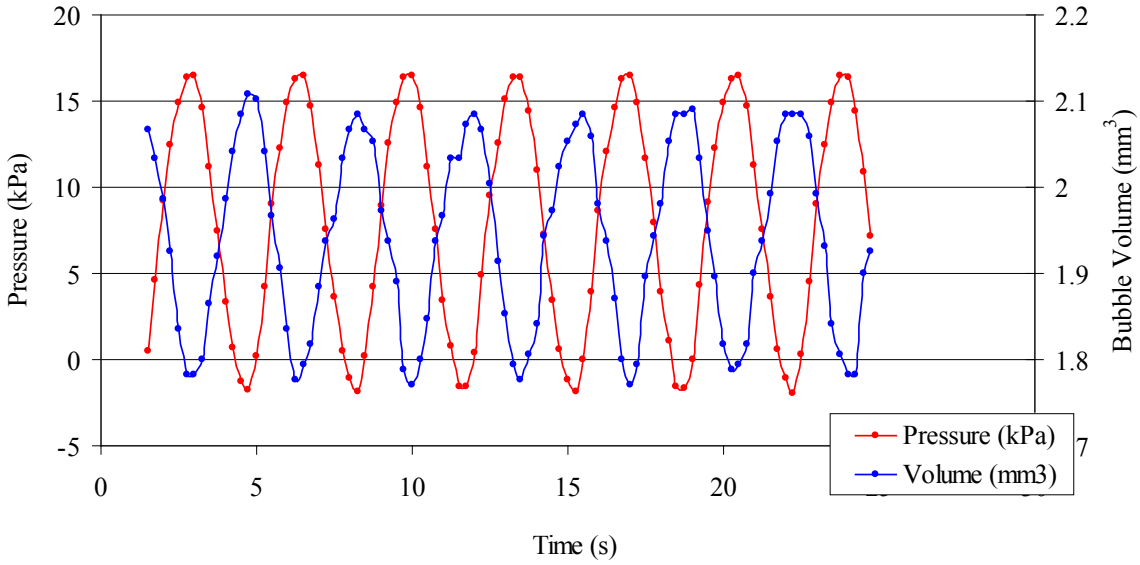

Fig. 5 Oscillation of bubble volume (blue line) responding to changes in wave-induced pressure oscillations (red line)

bubble and slower expansion when pressure was released (Fig. 6). This is explained with the friction forces that the expanding bubble has to overcome when pressure is reduced allowing the bubble to grow in size. The response of the bubble to the pressure oscillations is dependent on gas volume and decreases with decreasing bubble size (Fig. 6). This is explained with the reduction of the compressible gas volume.

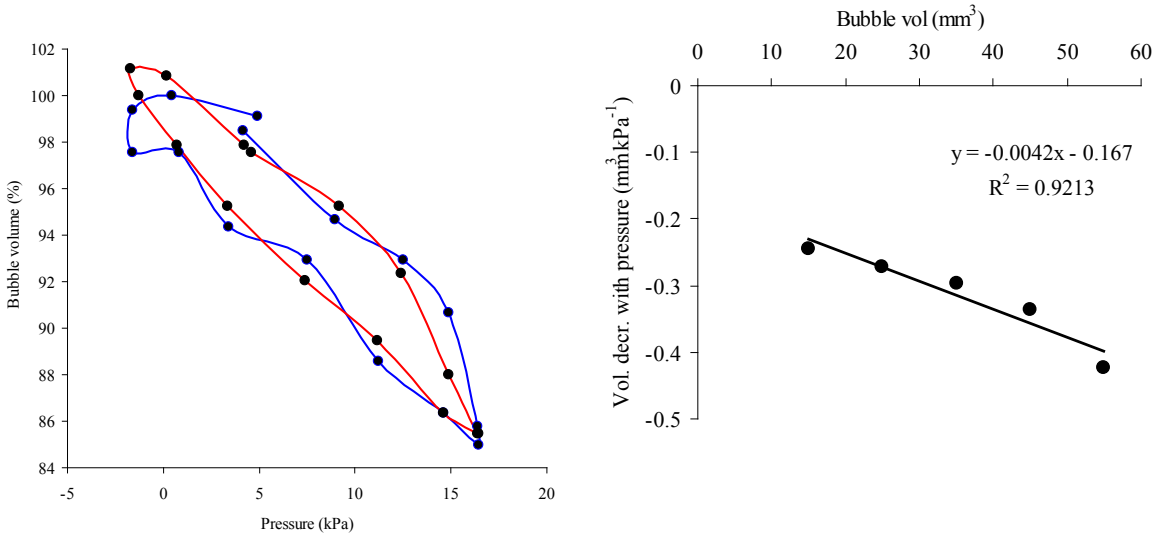

Fig. 6. Left graph: Hysteresis in small bubble volumes exposed to wave-induced pressure oscillations shown for two bubbles. Right graph: Dependency of pressure-related volume decrease on bubble volume.

Assessment of sedimentary bubble response to pressure oscillations
Gas bubbles embedded in saturated sand show a similar response to pressure oscillations as gas bubbles in the water column, however, the more rigid sand matrix doeas not permit uniform expansion of the gas bubble when expanding and gas moves into the pore space. This results in rough bubble surfaces that eventually form extrusions that penetrate further into the sediment forming cracks in the sediment matrix (Fig. 7).

Fig. 7. Compression of sedimentary bubble due to increasing pressure caused by a surface gravity wave. The picture with the upper bubble is superimposed to a picture of the same sediment cross section with the dilated bubble at low pressure (wave trough). Black lines are added to allow comparison of bubble diameter. The small bubble to the left shows similar change in size.

IMPACT/APPLICATIONS

The acoustic method we developed permits assessment of sound velocity in small volumes of water or sediment. This technique thus can be suitable for assessing sound propagation in samples retrieved from the sea floor where direct measurements are not possible. Sound propagation in sediments is important for evaluating sound reflection and scattering in sediments as caused by buried objects. With the mapping of small bubbles caused by benthic photosynthesis we demonstrate the usefulness of the developed technique for the scanning of shallow sediments for bubbles or other sediment heterogeneities. This allows the non-invasive characterization of sandy sediment surface layers at high spatial and temporal resolution, thereby permitting new insights of e.g. changes in sediment gas content during the day/night cycle or spatial distribution of embedded bubbles over a time period of a few hours. As these bubbles represent a reservoir of oxygen and thus a biogeochemical highly reactive electron acceptor, quantifying spatial and temporal distributions of bubbles is central for the understanding of the processes that govern biological, chemical and physical characteristics of the sediment surface layer. Determination of the volume and compotion of the bubbles released from coastal sediments allows assessing the potential effects on sediment acoustic and physical/biogeochemical characteristics. Information regarding the time period of bubble release from the sediment is essential for the interpretation of acoustic reflections from sediments and the evaluation of bubble effects on sediment characteristics. Our measurements of pressure effects on bubbles embedded in permeable sediments show that these bubbles pulsate when exposed to pressure oscillations caused by passing surface gravity waves. This influences water exchange processes.

TRANSITIONS

The project results on benthic oxygen production and bubble transport are relevant for benthic ecologist and oceanographers who seek a better understanding of the cycles of carbon and nutrients. The highly sensitive bubble detection method also may be applicable in medical sciences and industrial production processes. When operated by an underwater vehicle, this detection method may also be useful in detecting reflecting objects buried in the sand.

RELATED PROJECTS

NSF project "Further Development of the Eddy Correlation Technique; NSF-OCE-0536431; 01/01/06-12/31/10; $742,717; P. Berg, (PI), M. Huettel (co-PI). This project was awarded as a follow-up of our first eddy correlation project (OCE-0221159) and supported continuation of our research and instrument development related to the eddy correlation technique for the measurement of oxygen flux in permeable coastal sediment. In addition to intensive field campaigns at the two main field sites, the Virginia Coast Reserve LTER site and the Apalachicola NERR site, we have visited several other sites that appeared particularly challenging with respect to flux measurements. These include the rocky bottoms in The Great Lakes with dense colonies of the invasive Quagga mussel overgrown with filamentous algae and the deep ocean floor off the coast of Japan. Data from these sites have provided both new insights on benthic oxygen metabolism and a demonstration of the advantages of the eddy correlation technique in diverse environments.

REFERENCES

De Beer, D. and others 2005. Transport and mineralization rates in North Sea sandy intertidal sediments, Sylt-Romo Basin, Wadden Sea. Limnology and Oceanography **50:** 113-127.

Hefner, B. T., D. R. Jackson, K. L. Williams, and E. I. Thorsos. 2009. Mid- to High-Frequency Acoustic Penetration and Propagation Measurements in a Sandy Sediment. Ieee Journal of Oceanic Engineering **34:** 372-387.

Hines, P. C., J. C. Osler, J. G. E. Scrutton, and L. J. S. Halloran. 2010. Time-of-Flight Measurements of Acoustic Wave Speed in a Sandy Sediment at 0.6-20 kHz. Ieee Journal of Oceanic Engineering **35:** 502-515.

Huettel, M., and A. Rusch. 2000. Transport and degradation of phytoplankton in permeable sediment. Limnology & Oceanography **45:** 534-549.

Jansen, S., E. Walpersdorf, U. Werner, M. Billerbeck, M. E. Bottcher, and D. De Beer. 2009. Functioning of intertidal flats inferred from temporal and spatial dynamics of O-2, H2S and pH in their surface sediment. Ocean Dynamics **59:** 317-332.

Knobles, D. P., T. W. Yudichak, R. A. Koch, P. G. Cable, J. H. Miller, and G. R. Potty. 2006. Inferences on seabed acoustics in the East China Sea from distributed acoustic measurements. Ieee Journal of Oceanic Engineering **31:** 129-144.

Kuehl, M., and B. B. Joergensen. 1994. The light field of microbenthic communities: radiance distribution and microscale optics of sandy coastal sediments. Limnol. Oceanogr. **39:** 1368-1398.

Thorsos, E. I. and others 2001. An overview of SAX99: Acoustic measurements. Ieee Journal of Oceanic Engineering **26:** 4-25.

Turgut, A., and T. Yamamoto. 1990. Measurements of acoustic-wave velocities and attenuation in marine-sediments. Journal of the Acoustical Society of America **87:** 2376-2383.

Werner, U. and others 2006. Spatial and temporal patterns of mineralization rates and oxygen distribution in a permeable intertidal sand flat (Sylt, Germany). Limnology and Oceanography **51:** 2549-2563.

Wille, P. 2005. Sound Images of the Ocean: in Research and Monitoring Springer.

Williams, K. H. 2002. Monitoring Microbe-Induced Physical Property Changes Using High-Frequency Acoustic Waveform Data: Toward the Development of a Microbial Megascope. University Of California, Berkeley.

PUBLICATIONS

Wildman, Jr., R. A., Huettel, M. (submitted). Acoustic detection of gas bubbles in saturated sands at high spatial and temporal resolution.